

## Collapse of the $N = 28$ Shell Closure in $^{42}\text{Si}$

B. Bastin,<sup>2</sup> S. Grévy,<sup>1,\*</sup> D. Sohler,<sup>3</sup> O. Sorlin,<sup>1,4</sup> Zs. Dombrádi,<sup>3</sup> N. L. Achouri,<sup>2</sup> J. C. Angélique,<sup>2</sup> F. Azaiez,<sup>4</sup>  
D. Baiborodin,<sup>5</sup> R. Borcea,<sup>6</sup> C. Bourgeois,<sup>4</sup> A. Buta,<sup>6</sup> A. Bürger,<sup>7,8</sup> R. Chapman,<sup>9</sup> J. C. Dalouzy,<sup>1</sup> Z. Dlouhy,<sup>5</sup> A. Drouard,<sup>7</sup>  
Z. Elekes,<sup>3</sup> S. Franchoo,<sup>4</sup> S. Iacob,<sup>6</sup> B. Laurent,<sup>2</sup> M. Lazar,<sup>6</sup> X. Liang,<sup>9</sup> E. Liénard,<sup>2</sup> J. Mrazek,<sup>5</sup> L. Nalpas,<sup>7</sup> F. Negoita,<sup>6</sup>  
N. A. Orr,<sup>2</sup> Y. Penionzhkevich,<sup>10</sup> Zs. Podolyák,<sup>11</sup> F. Pougheon,<sup>4</sup> P. Roussel-Chomaz,<sup>1</sup>  
M. G. Saint-Laurent,<sup>1</sup> M. Stanoiu,<sup>4,6</sup> and I. Stefan<sup>1</sup>

<sup>1</sup>Grand Accélérateur National d'Ions Lourds (GANIL), CEA/DSM - CNRS/IN2P3, Bd Henri Becquerel,  
BP 55027, F-14076 Caen Cedex 5, France

<sup>2</sup>Laboratoire de Physique Corpusculaire, 6, bd du Mal Juin, F-14050 Caen Cedex, France

<sup>3</sup>Institute of Nuclear Research, H-4001 Debrecen, Pf.51, Hungary

<sup>4</sup>Institut de Physique Nucléaire, IN2P3-CNRS, F-91406 Orsay Cedex, France

<sup>5</sup>Nuclear Physics Institute, AS CR, CZ-25068 Rez, Czech Republic

<sup>6</sup>Institute of Atomic Physics, IFIN-HH, Bucharest-Magurele, P.O. Box MG6, Romania

<sup>7</sup>CEA Saclay, DAPNIA/SPHN, F-91191 Gif-sur-Yvette Cedex, France

<sup>8</sup>Helmholtz-Institut für Strahlen- und Kernphysik, Universität Bonn, Nußallee 14-16, D-53115 Bonn, Germany

<sup>9</sup>School of Engineering and Science, University of Paisley, PA1 2BE Paisley, Scotland, United Kingdom

<sup>10</sup>FLNR, JINR, 141980 Dubna, Moscow Region, Russia

<sup>11</sup>University of Surrey, GU2 7XH Guildford, United Kingdom

F. Nowacki<sup>12</sup> and A. Poves<sup>13</sup>

<sup>12</sup>IReS, BP28, F-67037 Strasbourg Cedex, France

<sup>13</sup>Departamento de Física Teórica, Universidad Autónoma de Madrid, E-28049 Madrid, Spain

(Received 20 December 2006; published 12 July 2007)

The energies of the excited states in very neutron-rich  $^{42}\text{Si}$  and  $^{41,43}\text{P}$  have been measured using in-beam  $\gamma$ -ray spectroscopy from the fragmentation of secondary beams of  $^{42,44}\text{S}$  at 39A MeV. The low  $2^+$  energy of  $^{42}\text{Si}$ , 770(19) keV, together with the level schemes of  $^{41,43}\text{P}$ , provides evidence for the disappearance of the  $Z = 14$  and  $N = 28$  spherical shell closures, which is ascribed mainly to the action of proton-neutron tensor forces. New shell model calculations indicate that  $^{42}\text{Si}$  is best described as a well-deformed oblate rotor.

DOI: [10.1103/PhysRevLett.99.022503](https://doi.org/10.1103/PhysRevLett.99.022503)

PACS numbers: 23.20.Lv, 21.60.Cs, 27.40.+z, 29.30.Kv

Magic nuclei have in common a high energy for the first excited state and a small transition probability  $B(E2: 0_1^+ \rightarrow 2_1^+)$  compared to neighboring nuclei. This is essentially due to the presence of large shell gaps, the origins and configurations of which differ significantly along the chart of nuclides. This implies a variable sensitivity of these shell gaps with respect to the proton-neutron asymmetry. For instance, the  $N = 20$  shell closure, bound by orbitals of opposite parity,  $d_{3/2}$  below and  $f_{7/2}$  above, remains remarkably rigid against quadrupole deformation from  $^{40}\text{Ca}$  to  $^{34}\text{Si}$  even after the removal of six protons [1]. This feature can be traced back to the large  $N = 20$  gap, the hindrance of  $2^+$  excitations due to the change of parity across it, and to the presence of proton subshell gaps in the  $sd$  shells at  $Z = 16$  ( $\sim 2.5$  MeV) and  $Z = 14$  ( $\sim 4.3$  MeV) [2,3]. Conversely, the  $N = 28$  shell closure, produced by the spin-orbit (SO) interaction and separating the orbitals of same parity  $f_{7/2}$  and  $p_{3/2}$ , is progressively eroded below the doubly magic  $^{48}\text{Ca}$  nucleus in  $^{46}\text{Ar}$  [4] and  $^{44}\text{S}$  [5,6], after the removal of only two and four protons, respectively. This rapid disappearance of rigidity of the  $N = 28$  isotones has been ascribed to the reduction of the neutron

shell gap  $N = 28$  combined with that of the proton subshell gap  $Z = 16$ , leading to increased probability of quadrupole excitations within the  $fp$  and  $sd$  shells for neutrons and protons, respectively. For the  $^{44}\text{S}$  nucleus, its small  $2^+$  energy, large  $B(E2)$  value [5], and the presence of a  $0_2^+$  isomer at low excitation energy [6] point to a mixed ground state configuration of spherical and deformed shapes. As the proton  $Z = 14$  and neutron  $N = 28$  (sub)shell gaps have been proven to be effective in  $^{34}_{14}\text{Si}$  and  $^{48}\text{Ca}_{28}$ , respectively, the search for a new doubly magic nucleus would be naturally oriented towards  $^{42}_{14}\text{Si}_{28}$ , which could be the lightest one with proton and neutron gaps created by the SO interaction.

The experimental status concerning the structure of  $^{42}\text{Si}$  is rather controversial. On the one hand the very short  $\beta$ -decay lifetimes of the  $^{40-42}_{14}\text{Si}$  nuclei point to deformed ground state configurations in the Si isotopic chain [7]. On the other hand, the weak two proton knockout cross section  $\sigma_{-2p}(^{44}\text{S} \rightarrow ^{42}\text{Si})$  was given as a strong indication in favor of a magic spherical nucleus [8] with a large  $Z = 14$  shell gap. However, the same authors have shown more recently [9] that a reduction of the  $Z = 14$  gap by as much as 1 MeV

does not increase the  $\sigma_{-2p}$  value significantly. Further, the newly measured atomic mass of  $^{42}\text{Si}$  [10] is compatible with an excess of microscopic energy as compared to a spherical liquid drop, which could be obtained either for a spherical or deformed shell closure.

The present work aimed at determining the  $2^+$  energy of  $^{42}\text{Si}_{14,28}$  and the energy spectrum of the neutron-rich  $^{41,43}\text{P}_{15,26,28}$  isotopes to obtain a global understanding of the proton and neutron excitations at  $Z = 14$  and  $N = 28$  to infer whether  $^{42}\text{Si}$  can be considered as a new doubly magic nucleus or not.

The experiment was carried out at the Grand Accélérateur National d'Ions Lourds (GANIL) facility. A primary beam of  $^{48}\text{Ca}$  at 60A MeV impinged onto a 200 mg/cm<sup>2</sup> C target with a mean intensity of 3.8  $\mu\text{A}$  to produce a cocktail of projectilelike fragments. They were separated by the ALPHA spectrometer, the magnetic rigidity of which was set to optimize the transmission of the  $^{44}\text{S}$  nuclei, produced at a rate of 125 s<sup>-1</sup>. Fragments were guided over a flight path of about 80 m along which the time of flight (TOF) was determined with two microchannel plates. A thin 50  $\mu\text{m}$  Si detector was used to determine the energy losses ( $\Delta E$ ), which completed the event by event identification prior to the fragmentation in a secondary target of 195 mg/cm<sup>2</sup> of  $^9\text{Be}$ . This target was placed at the entrance of the SPEG spectrometer, the magnetic rigidity of which was tuned to maximize the transmission of the  $^{42}\text{Si}$  nuclei produced through a 2 proton knockout reaction. At the focal plane of SPEG, ionization and drift chambers provided information on the  $\Delta E$  and positions of the transmitted nuclei, while a plastic scintillator was used to determine TOF and residual energies. The  $\sigma_{-2p}(^{44}\text{S} \rightarrow ^{42}\text{Si})$  cross section is measured to be 80(10)  $\mu\text{b}$  at 39A MeV. This agrees with the value of 120(20)  $\mu\text{b}$  obtained at 98.6A MeV [8], after having taken into account an enhancement factor of 25% due to the higher beam energy [11].

An array of 74 BaF<sub>2</sub> crystals, each of 9 cm diameter and 14 cm length, was arranged in two hemispheres above and below the Be target at a mean distance of 25 cm to detect  $\gamma$  rays arising from the secondary reactions. The energy threshold of the detectors was around 100 keV. The energies of two  $\gamma$  rays detected in coincidence in adjacent detectors were combined by addback. The  $\gamma$ -ray energies were corrected for Doppler shifts due to the in-flight emission by the fragments. Photopeak efficiencies of 38% at 779 keV, 24% at 1.33 MeV, and 16% at 2 MeV were achieved for fragments with  $v/c \approx 0.3$ . The energy resolution was 15% at 800 keV and 12% at 1.4 MeV, which includes the effects of the intrinsic resolution of the detectors and the Doppler broadening. Using the systematics of the peak widths deduced from the observation of known single peaks, doublets of  $\gamma$  rays could also be disentangled. The time resolution of the array was 800 ps. This enabled a clean separation between neutrons or charged particles and the  $\gamma$  rays arising from the reaction on the basis of their TOF differences.

$\gamma$ -ray spectra obtained for the  $^{42}\text{Si}$  and  $^{41,43}\text{P}$  isotopes are shown in Fig. 1. Several other nuclei were also produced, such as  $^{38,40}\text{Si}$  and  $^{44}\text{S}$ . Noteworthy is the fact that we find good agreement with their previously measured  $\gamma$  transitions, published in Refs. [5,12]. A clear single peak is visible in the spectrum of  $^{42}\text{Si}$  at 770(19) keV on a significance level of more than  $3\sigma$ . It can be assigned to the decay of the first excited state, namely, the  $2_1^+ \rightarrow 0_1^+$  transition. The number of counts corresponds to a feeding of the  $2^+$  state of  $44 \pm 10\%$ . In  $^{43}\text{P}$ , in addition to the low energy transition at 186 keV previously reported by Fridmann *et al.* [8], a doublet of weak transitions is visible at 789 and 918 keV. Both transitions are in coincidence with the 186 keV transition and are placed on top of it in the proposed level scheme (Fig. 2). In  $^{41}\text{P}$ , similarly to the  $^{43}\text{P}$  case, a strong low energy transition at 172(12) keV is visible together with several slightly overlapping peaks at 420, 964, 1146, and 1408 keV. The 964 and 1408 keV transitions are in coincidence with the 172 keV transition, while the 964 keV transition is in coincidence with that at 420 keV, too. In addition to coincidence relationships,

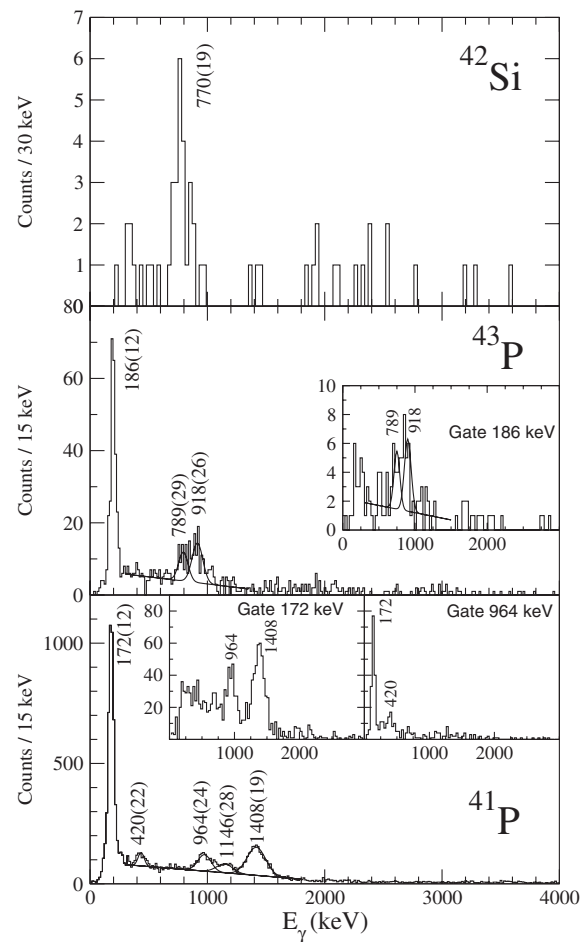


FIG. 1.  $\gamma$ -ray spectra observed in coincidence with the  $^{42}\text{Si}$  (upper),  $^{43}\text{P}$  (middle), and  $^{41}\text{P}$  (bottom) nuclei. In the insets  $\gamma$ - $\gamma$  coincidence spectra are presented, gated with transitions belonging to the  $^{41,43}\text{P}$  nuclei.

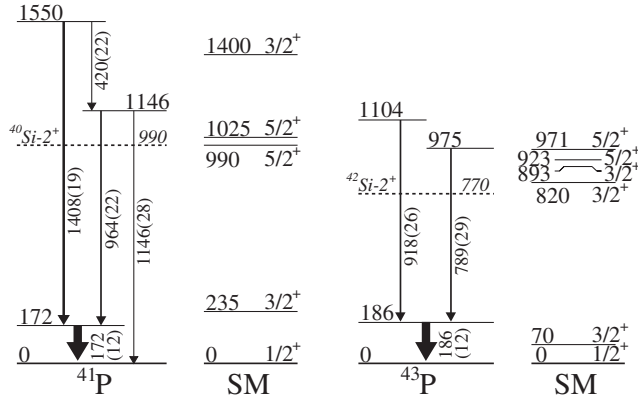


FIG. 2. Level schemes for  $^{41,43}\text{P}$  and the corresponding shell model calculations (SM) performed in the present work. Positions of the  $2^+$  states in  $^{40,42}\text{Si}$  are shown by dashed lines.

intensity arguments are used in order to build the level scheme presented in Fig. 2. The present observation of *new*  $\gamma$  lines in the  $^{43}\text{P}$  and  $^{42}\text{Si}$  is explained by an enhanced  $\gamma$  efficiency by about a factor of 10 at 1 MeV with respect to the work of Refs. [8,9].

Figure 3 shows the energies of the  $2^+$  states in the Si and Ca isotopes. The correlated increase of the  $2^+$  energies in the  $^{40}\text{Ca}$  and  $^{34}\text{Si}$  nuclei at  $N = 20$  does not hold at  $N = 28$ . While  $2^+$  energies increase in Ca isotopes from  $N = 24$  to reach a maximum around 4 MeV at  $N = 28$ , the  $2^+$  energies in the Si isotopes start to deviate from those of the Ca at  $N = 26$ , reaching a minimum value at  $N = 28$ . The slight deviation from the Ca curve at  $N = 26$  was interpreted in Ref. [12] as an indication in favor of a reduced  $N = 28$  shell gap. However, neutron excitations occurring *before* the complete filling of the  $\nu f_{7/2}$  shell are not especially sensitive to the  $N = 28$  gap, as the  $2^+$  states are qualitatively due to excitations *inside* the  $f_{7/2}$  shell. Conversely, in  $^{42}\text{Si}_{28}$  the  $2^+$  state comes from particle-hole excitations across the gap and therefore, the dramatic decrease of its  $2^+$  energy leaves no doubt concerning the disappearance of the spherical  $N = 28$  shell closure at  $Z = 14$ , the energy of 770 keV being one of the smallest among nuclei having a similar mass. It is worth pointing out, as

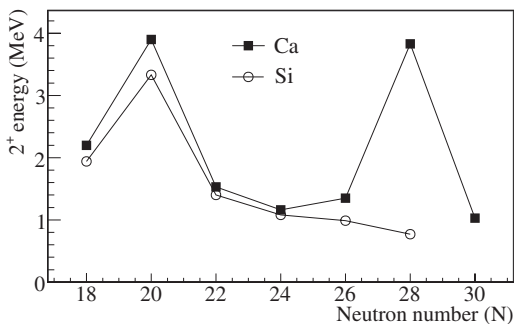


FIG. 3. Energies of the  $2^+$  states measured in the Ca and Si isotopes. Present result for  $^{40,42}\text{Si}$ —770(19) keV—brings evidence for the collapse of the  $N = 28$  shell closure at  $Z = 14$ .

shown in Fig. 2, that the decrease of the  $2^+$  energies in the  $^{40,42}\text{Si}$  nuclei is correlated to the behavior of those states observed around 1 MeV in the  $^{41,43}\text{P}$  isotones, which in the shell model arise from the coupling of the last proton in the  $s_{1/2}$  or  $d_{3/2}$  orbitals to the  $2^+$  excitation. This provides additional support to the disappearance of the  $N = 28$  spherical gap. If the  $N = 28$  gap had persisted in the P isotopes, a sequence of levels similar to those in  $^{47}\text{K}$  would have been observed, namely two nearby  $1/2^+$  and  $3/2^+$  states originating from the quasidegeneracy of the  $\pi s_{1/2}$  and  $\pi d_{3/2}$  orbitals and a large gap in energy ( $\sim 2$  MeV) above this doublet.

The spectroscopy of the nuclei with proton number in the range of 16 to 20 and neutron number from 20 to 28 is reproduced successfully when using large scale shell model calculations in a valence space comprising the full  $sd$  shells for protons and  $pf$  shells for neutrons with the effective interaction SDPF-NR [13]. The remarkable features of this interaction which account for the evolution of the nuclear structure between  $N = 20$  and  $N = 28$  are (i) the decrease of the  $d_{3/2}-s_{1/2}$  proton splitting by about 2.5 MeV from  $^{39}\text{K}_{20}$  to  $^{47}\text{K}_{28}$  as the neutron  $f_{7/2}$  orbital is filled and (ii) the reduction of the  $N = 28$  gap by about 330 keV per pair of protons [4] removed from the  $^{48}\text{Ca}$ .

Despite these successes, a correct description of the Si isotopes cannot be straightforwardly obtained by using the monopole matrix elements of the SDPF-NR interaction derived for the Ca isotopes. This arises from the fact that the occupied and valence proton orbitals involved in both cases are somewhat different. In particular, some amount of core excitations to the  $\pi f_{7/2}$  orbital, which lies just above the valence space of the Ca isotopes, is included in the neutron-pairing matrix elements  $V^{nn}$  of  $pf$ -shell orbits. This contribution is expected to be negligible in the Si isotopes, in which the  $\pi f_{7/2}$  orbital lies at much higher excitation energy. According to the model, the configuration of the  $2^+$  states in  $^{36,38,40}\text{Si}$  arises mainly from pair-breaking inside the  $\nu f_{7/2}$  shell and therefore the  $2^+$  energies scale with the  $V^{nn}$  values. Indeed the energy of the  $2^+$  states in  $^{36,38,40}\text{Si}$  [1,12,14] and those of the  $5/2^+$  states in  $^{37,39}\text{P}$  [15] are overestimated by the SDPF-NR interaction up to 300–400 keV. The discrepancy is larger for  $^{42}\text{Si}$ , the calculated  $2^+$  energy of which being 1.49 MeV, instead of 770 keV. Therefore, a reduction of the  $pf$  shell  $V^{nn}$  matrix elements by 300 keV gives the  $2^+$  energies of  $^{36,38,40}\text{Si}$  as well as the  $5/2^+$  energies in  $^{37,39}\text{P}$  [15] in agreement with their experimental values. Nevertheless the calculated  $2^+$  energy in  $^{42}\text{Si}$ , 1.1 MeV, is still larger than the experimental value. To further reduce it without changing the properties of the other  $N = 28$  isotones, the proton-neutron monopole matrix elements  $V_{d_{5/2}(fp)}^{pn}$  can be considered. Indeed, the  $d_{5/2}$  orbital is “active” in the Si isotopes whereas it is too deeply bound to play a significant role in the description of the Ca isotopes. Nevertheless, with the SDPF-NR interaction the proton  $d_{3/2}-d_{5/2}$  splitting in  $^{39}\text{K}$  and  $^{47}\text{K}$  overestimates the experimental values, see Table I.

TABLE I. Proton  $d_{3/2}$ - $d_{5/2}$  splitting in  $^{39}\text{K}$  and  $^{47}\text{K}$ .

	$^{39}\text{K}$	$^{47}\text{K}$
Experiment	6.74 [2]	4.84 [16]
Shell model [13]	7.4	5.92
Shell model (this work)	7.18	4.93

By modifying adequately the  $V_{d_{5/2}(fp)}^{pn}$  matrix elements, the  $d_{3/2}$ - $d_{5/2}$  splitting can be better adjusted in the K isotopes (Table I) and therefore the  $2^+$  energies in  $^{36,38,40,42}\text{Si}$ , as well as the level schemes of  $^{41,43}\text{P}$ , agree nicely with the experimental data shown in Figs. 2 and 3. This modification leads to a decrease of the  $d_{3/2}$ - $d_{5/2}$  splitting by 1.94 MeV from  $^{34}\text{Si}$  to  $^{42}\text{Si}$  which results in an enhanced collectivity.  $^{42}\text{Si}$  becomes clearly an oblate rotor up to  $J = 8^+$ ; with a calculated  $2^+$  excitation energy of 810 keV and an intrinsic quadrupole moment  $Q_i$  of  $-87e\text{ fm}^2$  corresponding to a quadrupole deformation  $\beta = -0.45$ . The doubly magic ( $N = 28$ ,  $Z = 14$ ) component is only 20% of the ground state wave function with an average 2.2 neutrons above  $N = 28$  and 1.2 protons above  $Z = 14$ ; the percentage of the closed proton configuration  $(0d_{5/2})^6$  being 33%. With a present  $Z = 14$  gap of 5.8 MeV, our measured  $\sigma_{-2p}(^{44}\text{S} \rightarrow ^{42}\text{Si})$  cross section agrees with the one calculated with a similar gap in Ref. [9].

The resulting shell model description of the  $N = 20$  to  $N = 28$  region south of Ca isotopes is the following: as compared to the  $^{34}\text{Si}$  and  $^{48}\text{Ca}$  nuclei, major changes in the energies of the proton and neutron orbitals are occurring towards  $^{42}\text{Si}$ . The complete filling of the neutron  $f_{7/2}$  shell from  $^{34}\text{Si}$  leads to a shrinkage of the  $sd$  orbitals, with a proton SO splitting  $d_{3/2}$ - $d_{5/2}$  reduced by about 1.94 MeV. This reduction is compatible with what is accounted for by tensor forces, which act attractively (repulsively) between the proton and neutron orbits  $d_{3/2}$ - $f_{7/2}$  ( $d_{5/2}$ - $f_{7/2}$ ) as described in Refs. [17,18]. Simultaneously, as depicted in Ref. [4] the removal of protons from  $^{48}\text{Ca}$  induces a compression in energy of the four neutron  $fp$  orbits and hence a reduction of the  $N = 28$  gap by about 1 MeV in  $^{42}\text{Si}$  (from an initial value of 4.8 MeV in  $^{48}\text{Ca}$ ) due to the combined effects of the proton-neutron tensor force and the density dependence of the SO interaction. The overall picture would be then that the mutual actions of the proton-neutron tensor forces in  $^{42}\text{Si}$  induce the reduction of the neutron  $N = 28$  gap and limit the size of the proton  $Z = 14$  gap. In addition, particle-hole excitations between occupied and valence orbitals which are separated by  $\Delta\ell$ ,  $j = 2$  for both protons ( $sd$ ) and neutrons ( $fp$ ) naturally favor quadrupole correlations that generate collectivity through mechanisms related to Elliott's SU(3) symmetry [19]. The combined effects of the compression of the proton and neutron orbitals, plus the quadrupole excita-

tions, produce a rich variety of behaviors and shapes in the even  $N = 28$  isotones; spherical  $^{48}\text{Ca}$ ; oblate noncollective  $^{46}\text{Ar}$ ; coexistence in  $^{44}\text{S}$ , and two rotors, oblate  $^{42}\text{Si}$  and prolate  $^{40}\text{Mg}$ . This variety of shapes is also globally supported by mean field calculations, relativistic or nonrelativistic [20–24].

To summarize, the energies of excited states in the  $^{42}\text{Si}$  and the  $^{41,43}\text{P}$  nuclei have been measured through in-beam  $\gamma$ -ray spectroscopy. The low energy of the  $2_1^+$  state in  $^{42}\text{Si}$ , 770(19) keV, together with the level schemes of  $^{41,43}\text{P}$ , provides evidence for the disappearance of the  $N = 28$  shell closure around  $^{42}\text{Si}$ . It is ascribed to the combined action of proton-neutron tensor forces leading to a global compression of the proton and neutron single particle orbits, added to the quadrupole symmetry between the occupied and valence states which favors excitations across the  $Z = 14$  and  $N = 28$  shell gaps.

This work benefits from discussions with A. Navin, J. Tostevin, and L. Gaudefroy. The authors are thankful to the GANIL and LPC staffs. We thank support by BMBF No. 06BN109, GA of Czech Republic No. 202/040791, MEC-DGI-(Spain) No. BFM2003-1153, and by the EC through the Eurons Contract No. RII3-CT-3/2004-506065 and OTKA No. T38404-T42733-T46901. R.B., A.B., M.L., S.I., F.N. and R.C., X.L. acknowledge the IN2P3/CNRS and EPSRC support.

\*Corresponding author.

grevy@in2p3.fr

- [1] R. W. Ibbotson *et al.*, Phys. Rev. Lett. **80**, 2081 (1998).
- [2] P. Doll *et al.*, Nucl. Phys. **A263**, 210 (1976).
- [3] C. E. Thorn *et al.*, Phys. Rev. C **30**, 1442 (1984).
- [4] L. Gaudefroy *et al.*, Phys. Rev. Lett. **97**, 092501 (2006).
- [5] T. Glasmacher *et al.*, Phys. Lett. B **395**, 163 (1997).
- [6] S. Grévy *et al.*, Eur. Phys. J. A **25**, s1.111 (2005).
- [7] S. Grévy *et al.*, Phys. Lett. B **594**, 252 (2004).
- [8] J. Fridmann *et al.*, Nature (London) **435**, 922 (2005).
- [9] J. Fridmann *et al.*, Phys. Rev. C **74**, 034313 (2006).
- [10] B. Jurado *et al.*, Phys. Lett. B **649**, 43 (2007).
- [11] J. Tostevin (private communication).
- [12] C. M. Campbell *et al.*, Phys. Rev. Lett. **97**, 112501 (2006).
- [13] E. Caurier *et al.*, Nucl. Phys. **A742**, 14 (2004).
- [14] X. Liang *et al.*, Phys. Rev. C **74**, 014311 (2006).
- [15] O. Sorlin *et al.*, Eur. Phys. J. A **22**, 173 (2004).
- [16] G. J. Kramer *et al.*, Nucl. Phys. **A679**, 267 (2001).
- [17] A. Gade *et al.*, Phys. Rev. C **74**, 034322 (2006).
- [18] T. Otsuka *et al.*, Phys. Rev. Lett. **95**, 232502 (2005).
- [19] Elliott *et al.*, Proc. R. Soc. A **245**, 128 (1958).
- [20] G. A. Lalazissis *et al.*, Phys. Rev. C **60**, 014310 (1999).
- [21] S. Péru *et al.*, Eur. Phys. J. A **9**, 35 (2000).
- [22] R. Rodríguez-Guzmán *et al.*, Phys. Rev. C **65**, 024304 (2002).
- [23] T. R. Werner *et al.*, Nucl. Phys. **A597**, 327 (1996).
- [24] P.-G. Reinhard *et al.*, Phys. Rev. C **60**, 014316 (1999).